Interface roughness and the dispersion of confined LO phonons in GaAs/AlAs quantum wells

G. Fasol,*
Institute of Industrial Science, University of Tokyo, 7-22-1 Roppongi, Minato-ku, Tokyo 106, Japan and Frontier Research Programme, The Institute for Physical and Chemical Research (RIKEN), 2-1 Hirasawa, Wako-Shi, Saitama 351-01, Japan

M. Tanaka and H. Sakaki
Institute of Industrial Science, University of Tokyo, 7-22-1 Roppongi, Minato-ku, Tokyo 106, Japan

Y. Horikoshi
NTT Electrical Communications Laboratories, Musashino-shi, Tokyo 180, Japan
(Received 21 March 1988)

We report the energies of the confined LO phonon modes in the GaAs wells of GaAs/AlAs superlattices with well widths between 10 and 18 monolayers. We observe confined LO-phonon modes up to 12th order. The measurements were performed on sample structures obtained by two different growth techniques [molecular-beam epitaxy (MBE) with growth interruption and migration-enhanced epitaxy (MEE)], which favor the smoothness of the GaAs/AlAs and the AlAs/GaAs interfaces. Measurements on a sample, where the "normal" GaAs/AlAs interfaces were grown on purpose without growth interruption, show weaker Raman signals and confined phonon modes up to lower order than observable for samples with growth interruption. The energies of the confined LO phonons as a function of the confinement wave vector lie close to recent neutron results for the LO-phonon dispersion in bulk GaAs. We suggest that previously reported discrepancies are due to stronger interface roughness than in the present samples. We show that the high-order confined phonons are considerably more sensitive to roughness than the low-order confined LO phonons. Therefore the former and not the latter should be used for characterization of interface roughness. For determination of the phonon dispersion, on the other hand, the uncertainties are higher for the higher-order confined modes. We observe discrete confined modes corresponding to sections of the quantum well with thicknesses differing by one monolayer.

I. INTRODUCTION

Phonons in semiconductor superlattices have recently attracted much attention and several reviews summarize their properties.[1-4] Phonons in layered structures have interesting new properties: In specific energy regions they may be described by "folding" into the reduced Brillouin zone.[5,6] In other energy regions phonons may be localized in some of the layers, leading to a description in terms of slab modes.[7,8] In addition, different types of interface related phonons have been observed[9] and predicted.[10]

The present work is concerned with confined phonons. A superlattice consisting of alternating layers of material A and material B has ranges of phonon energy, where particular phonon branches of material A and of material B overlap. In those regions the phonons are propagative parallel to the growth direction of the lattice, and the resulting phonon modes are described by folding of the phonon branches into the reduced Brillouin zone.[5,6] In those energy regions, where the phonon branches do not overlap, the phonons remain confined in material A or B. In a force-constant model the strength of the confinement is determined by the ratio of the reduced masses and by the force constants in the two materials. In the case of GaAs/AlAs quantum wells, the mass of the Ga atoms ($m=70$) and the Al atoms ($m=27$) is so dramatically different that the confinement is abrupt to within one monolayer, i.e., the situation of the optical phonons may be described by the eigenmodes of clamped slabs of GaAs or AlAs, respectively.[8,11,13]

A $GaAs_N/AlAs_M$ superlattice of wells with N monolayers of GaAs and M monolayers of AlAs has N discrete LO_{GaAs} modes, N discrete TO_{GaAs} modes, both confined almost abruptly to the GaAs well. There are M discrete LO_{AlAs} and M discrete TO_{AlAs} modes, confined almost abruptly to the AlAs barriers. The phonon confinement results from the fact that the optical-phonon branches in GaAs and in AlAs do not overlap as a consequence of the large difference of the reduced masses of both materials. The confined phonon modes have dispersion parallel to the quantum-well plane, which has been calculated recently by Ren, Chu, and Chang[14] and by Richter and Strauch.[15]

Jusserand and Paquet[16] remarked that the well thickness relevant for the confinement of the phonons is larger than the "stoichiometric" thickness. In the layer sequence

... Al As Al As Al As* Ga As Ga As Ga
As Ga As Ga As* Al As Al As Al As...

the GaAs well stoichiometrically contains five Ga atoms and five As atoms. The As atoms at the edges, marked with an asterisk, are exactly equivalent with respect to lattice vibrations. Therefore the well thickness for phonon confinement is one monolayer larger than the

"stoichiometric" layer thickness.

Understanding phonons in quantum wells and superlattices is of fundamental importance. They are not only interesting in their own right. Raman measurements of the energies of confined phonons in quantum wells may be used as an alternative to neutron scattering determinations of the phonon dispersion.[8,11,16–18] Secondly, Raman measurements of phonon modes have been used for the characterization of the broadening of interfaces due to heat-induced interdiffusion[19,20] and of interface roughness.[21] Thirdly, the electron-phonon interaction is an important energy-loss mechanism and scattering mechanism in quantum-well devices.

In the present paper we study the influence of interface roughness on the confined LO phonons in GaAs/AlAs quantum wells, with well thicknesses of 10 and 17 monolayers. We study GaAs/AlAs quantum-well samples grown with refined molecular beam epitaxy (MBE) with growth interruption at the interfaces[22] and with the novel migration enhanced epitaxy (MEE).[23,24] We show that the absence of growth interruption in the case of MBE has a pronounced effect on the Raman spectra of confined phonons. We examine the influence of interface roughness in high-quality quantum wells on the determination of the phonon dispersion. We show that high-order confined LO-phonon modes are much more sensitive to interface roughness than the low-order confined phonon modes. Therefore, low-order confined phonon modes should be used for determination of the phonon dispersion with Raman scattering in superlattices. On the other hand, the high-order phonon modes should be used if information on interface roughness is desired. By considering the different importance of interface roughness on low- and high-order confined phonon modes, we find a natural explanation for the discrepancies between Raman determination and neutron determination of the phonon dispersion, which appears for the high-order confined phonon modes in previous work.[16–18] We note that we do not find evidence for Raman signals from the dielectric interface modes[9] in our samples.

II. CHARACTERIZATION OF MBE AND MEE QUANTUM WELLS

The properties of the GaAs/AlAs quantum wells are summarized in Table I. These quantum wells have thicknesses between 7 and 17 monolayers. Some were grown at 580 °C by refined MBE techniques using growth interruption for 90 s for the interfaces to improve their smoothness (type *A* of Ref. 25). One sample was examined for which the growth was interrupted for the bottom AlAs/GaAs interface but *not interrupted* for the top GaAs/AlAs interface (type *C* of Ref. 25). Another sample has been prepared by a novel MBE technique termed migration enhanced epitaxy (MEE).[23,24] During MEE growth the molecular beams of Ga (or Al) and As during the growth process are alternatively supplied such that the migration of the molecules along the growth surface is enhanced leading to smoother interfaces.[23,24] The substrate temperature during MEE growth is 300 °C, which is radically lower than conventional MBE growth.

Figure 1 shows luminescence spectra (dotted curves) and luminescence excitation spectra (solid curves) for four of the present samples. The samples 1 and 3 have been produced using refined MBE with growth interruption at both top and bottom interfaces. Sample 2 has been produced using MEE. One of the purposes of this figure is to show the extremely narrow luminescence spectra of the present samples, which have extremely smooth interfaces. For comparison, the luminescence spectra of sample 4 are shown. This sample has been grown with growth interruption only at the bottom interface—the top interface has been grown continuously. Sample 4 shows luminescence peaks which are about

TABLE I. Parameters of the GaAs/AlAs multiple-quantum-well samples.

Sample number	Well thickness (monolayers)	Barrier thickness (monolayers)	Number of periods (monolayers)	Growth details	Growth temp. (°C)
1	17	18	5	MBE, interruption at both interfaces (type *A*)	580
2	17	17	50	MEE	300
3	17	21	50	MBE, interruption at both interfaces (type *A*)	580
4	17	18	5	MBE, interruption only at bottom interface (type *C*)	580
5	10	10	40	MBE, interruption at both interfaces (type *A*)	600

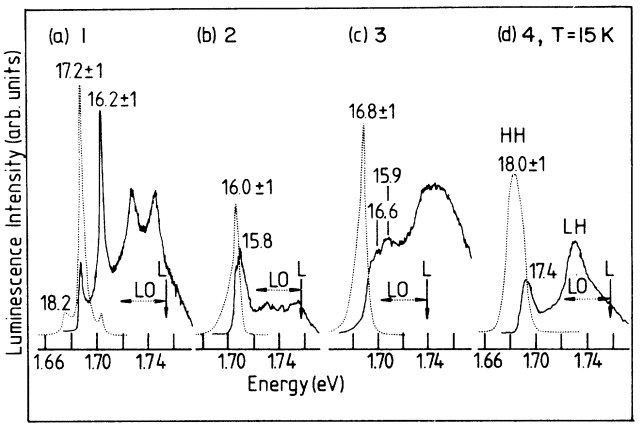

FIG. 1. Luminescence and luminescence excitation spectra for four of the samples studied in this paper. (a) Sample 1, (b) sample 2, (c) sample 3, (d) sample 4. The numbers above the luminescence features indicate the corresponding well thicknesses in units of monolayers (2.83 Å)—see text. The numbers are not integers, due to the pseudosmoothness of the bottom interface of the wells. Also shown is the laser frequency for the Raman measurements (indicated by symbol L) and the energy one LO-phonon energy below to show the position of the Raman spectra. The conditions are close to double resonance.

4.5 times broader than samples 1, 2, and 3, which are grown with the mentioned advanced techniques.

Samples 1, 2, and 3 have luminescence half widths as narrow as 3.5, 6, and 7 meV, respectively, which confirms the excellent quality of these quantum wells. These luminescence band widths are very much smaller than those of conventionally grown wells of the same width. Thus Fig. 1 shows that sample 4 (without growth interruption at the top interface) shows a luminescence width of 16 meV. Growth interruption at the top interface leads to a luminescence spectrum, which is a factor 4.5 narrower. We will show below that these different interface properties are also reflected in the phonon spectra. In both luminescence and luminescence excitation spectra of sample 1 we observe a series of sharp peaks. They correspond to sections of the sample with well thicknesses differing by exactly one monolayer. These sections may be situated within one and the same well, or it may also be sections in different parallel wells. It was shown previously, that these one monolayer steps occur in the top (GaAs/AlAs) interface,[25,26] while the bottom (AlAs/GaAs) interface is pseudosmooth, i.e., the interface has steps with a coherence length shorter than the exciton Bohr radius. There is no Stokes shift between luminescence peaks and the corresponding luminescence excitation peaks for sample 1. Samples 2, 3, and 4 have Stokes shifts of 2.5, 12, and 10 meV, respectively. In the case of samples 2, 3, and 4 the determination of the Stokes shift is not unique, since the luminescence peaks corresponding to different well thicknesses spaced by one monolayer, as in sample 1, have not been observed.

The thicknesses of the present quantum wells was controlled as accurately as possible during growth by observing the reflection high-energy electron diffraction (RHEED) oscillations, by luminescence and luminescence excitation spectroscopy. In addition, the well thickness was determined for several samples by electron microscopy. The thicknesses determined in this way are shown in Table I. It is generally accepted that present-day MBE techniques lead to a pseudosmooth AlAs/GaAs bottom interface and a "smooth" GaAs/AlAs top interface as a consequence of the different surface diffusion of the molecules participating in the growth. These conclusions result from luminescence measurement and from other measurements. The length scale of the interface fluctuations separating smooth and pseudosmooth is found to be of the order of the exciton radius. To the best of our knowledge all interfaces produced so far have a roughness amplitude of around one monolayer per interface in the best samples. The coherence length of the roughness (i.e., the extension of the perfectly smooth sections of the top interface) can be of the order of many micrometers in the best samples. Therefore, progress in accurate determination of the electronic structure of short period superlattices is limited by thickness fluctuations due to interface roughness. Even though x-ray measurements can determine the thickness of a quantum well averaged over the cross section of the x-ray beam with great accuracy, the thickness fluctuation remains. Not surprisingly therefore, available measurements and calculations of the lowest exciton energy as a function of well thickness show scatter corresponding to a thickness fluctuation of plus or minus one monolayer.

Some recent experimental results[27–31] for the lowest exciton luminescence energy as a function of well thickness are shown in Fig. 2 for short-period superlattices

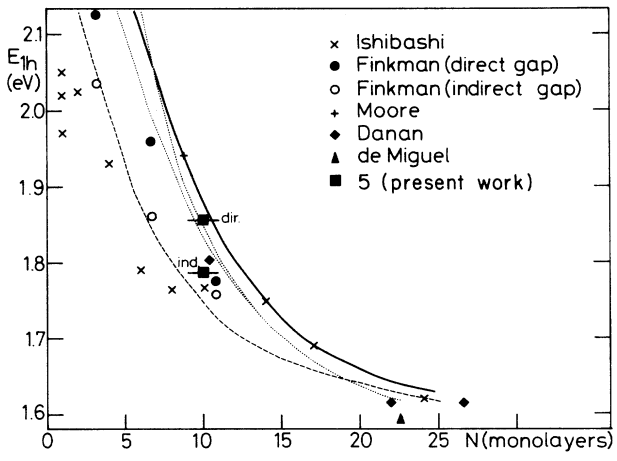

FIG. 2. Energy of lowest exciton luminescence peak as a function of thickness (measured as number N of monolayers) for $GaAs_N/AlAs_N$ quantum wells. Experimental data are from Ishibashi *et al.* (Ref. 27), Finkman *et al.* (Ref. 28), Moore *et al.* (Ref. 29), Danan *et al.* (Ref. 30), de Miguel *et al.* (Ref. 31), and from the present work. The solid line represents Kronig-Penney calculations from Ref. 28, the dashed line is a tight binding calculation (Ref. 32), whereas the dotted line is calculated by the present authors following work by Bastard (Ref. 33) and using the parameters shown in Table II. Our calculation only takes into account band contributions that are near Γ. The calculation shown with the dotted line indicates the width of the miniband as the splitting below $N < 13$.

with equal widths of GaAs well and AlAs barriers. We have also included data for our sample 5, where the error bar reflects the well thickness uncertainty due to the interface roughness. Figure 2 also shows the results of a Kronig-Penney calculation[28] (solid line), of a tight-binding calculation[32] (dashed line), and of an envelope-function calculation, which we have done, based on Bastard's method[33] (dotted line). This latter calculation also shows the limits of the minibands, due to overlap of the wave functions in different wells. The parameters we have used for this calculation are given in Table II. We have used the determination of Finkman *et al.*,[28] shown as the solid line in Fig. 2, to determine the well thickness for each particular luminescence energy. We should keep in mind, that in our opinion, there is an uncertainty of plus or minus one monolayer in all well-thickness determinations representing the state of the art in sample growth and characterization. This uncertainty is represented by error bars in the other figures of this work. The thicknesses determined in this way are shown in Fig. 1 above the luminescence peaks and they agree well with the growth data in Table I.

III. EXPERIMENTAL TECHNIQUES

Raman measurements of the confined LO_{GaAs} phonon modes and the luminescence and luminescence excitation measurements for characterization were performed at 15±2 K (measured with a carbon-glass resistor behind the sample) in a closed-cycle Helium refrigerator. Due to the heating of the sample by the laser, the sample temperature is slightly higher by around 1 or 2 °C. We used a conventional photon counting Raman system with a 1-m double monochromator, an Argon-ion laser, and a dye laser with appropriate laser dyes. Most measurements were done with line focus. Some measurements were done with a point focus (with low laser power to avoid heating) to select a favorable region of the sample structure and to investigate the spatial variation of the luminescence and the Raman spectra across the sample structures. Luminescence and luminescence excitation measurements were done on the same spot as the Raman measurements for calibration.

TABLE II. Parameters used for the envelope function calculation.

	Band offsets (eV)	
Conduction band	1.112	
Valence band	0.500	
Split-off band	0.434	
	GaAs	AlAs
Energy gap E_0 (eV)	1.519	3.13
Spin splitting Δ_0 (eV)	0.340	0.275
Effective masses		
m_e/m_0	0.066	0.15
$m_{hh\perp}/m_0$	0.377	0.478
$m_{lh\perp}/m_0$	0.0905	0.208
k·p matrix element (eV)		
$2m_0(\langle s \mid p_x \mid x \rangle/m_0)^2$	24.26	24.26

Most Raman measurements were done close to the lowest exciton energy. Figure 1 shows the energies of the laser light used for the Raman measurements for four of the samples studied and indicates the energy range of the Raman spectra. The energies shown correspond to the position most favorable for the experiment, i.e., strongest ratio of Raman signal to noise of the background luminescence. Clearly the outgoing beam is close to the heavy-hole exciton in that thickness region dominating the luminescence excitation spectrum. In addition, the incident laser beam used for Raman scattering is close to the light-hole exciton energy. Therefore, our conditions are close to double resonance.[34–36] This is supported by the agreement of our polarization dependence results (reported below) with those of Ref. 35. We have studied the polarization dependence of the Raman spectra using prism polarizers and polarization rotators for the incident and scattered laser beam. The samples were mounted in the cryostat in an orientation such that in each case the polarization vector was parallel to a [100] direction. The directions in the plane of the well are defined as $x \| [100]$ and $y \| [010]$, while $z \| [001]$ is perpendicular to the wells.

IV. CONFINED LO PHONONS IN THE GaAs WELLS

Figures 3–5 show selected Raman spectra of the confined LO-phonon modes in several of the samples

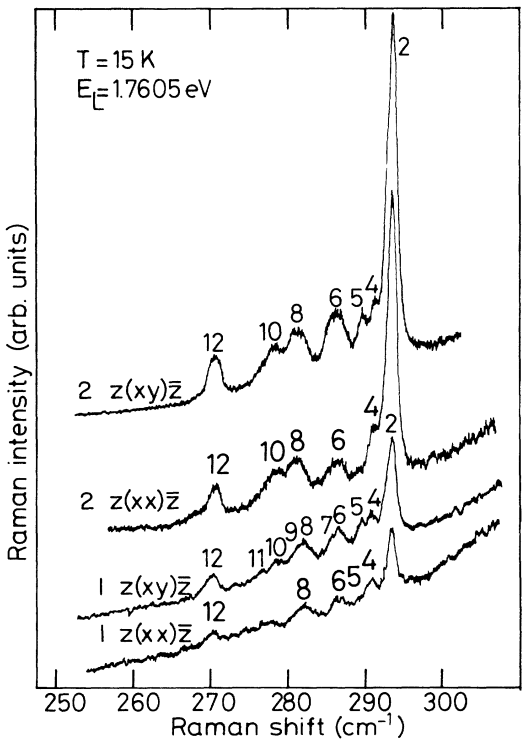

FIG. 3. Raman spectra of the confined LO_{GaAs} phonons in the GaAs/AlAs quantum-well samples 2 and 1. Spectra are shown both for parallel polarization $[z(x,x)\bar{z}]$ and for crossed polarization $[z(x,y)\bar{z}]$. Measurements are taken at 15±2 K. The selection rules agree with those for double resonance.

which we have studied. In Fig. 3 we show Raman spectra of sample 1, grown by refined MBE using growth interruption at both top and bottom interfaces. We also show spectra of sample 2, grown by the MEE technique. We see that in each case several Raman peaks due to confined LO-phonon modes are observed. We find that the Raman signals for both samples are stronger in the case of $z(x,y)\bar{z}$ polarization than in the case of $z(x,x)\bar{z}$ polarization. This situation is well explained by the fact that we have double resonance, i.e., resonance of both the incoming and outgoing Raman photon with electronic excitations of the sample, as shown in Fig. 1. The polarization-dependence results shown in Fig. 3 agree with the results of Ref. 35. By comparison of these Raman spectra with spectra taken with higher laser energies including the 5145-Å Argon-ion laser line, we can assign these Raman peaks to confined LO_n phonon modes. The assignment of the order n is indicated in Fig. 3. The situation here is different than in the case of Sood *et al.*[8] due to the double resonance. Thus we also find deformation-potential coupling to the $n=5$ mode for crossed polarization $z(x,y)\bar{z}$. The spectra of the confined LO-phonon modes in samples 1 and 2 are very similar—the main difference is the increased width of the modes $n=8$ and $n=10$ in sample 2. This point will be discussed later in this paper. Raman scattering from the TO-phonon mode is excluded in this configuration due to the selection rules.

Figure 4 shows Raman spectra from confined LO phonons in samples 1, 2, 3, and 4. Sample 4 is grown without interruption of the growth at the top interface: The LO-phonon Raman spectra are broader, the Raman intensity is considerably lower at the best resonance we could obtain, and Raman peaks for orders higher than $n=10$ are absent. There is a shoulder on both sides of the LO-phonon peak for $n=2$. On the low-energy side, this peak will be caused by the $n=4$ phonon, but on the high-energy side it will either be due to the $n=1$ peak or by contributions from phonons in well regions with strongly different confined LO-phonon energy. Samples 1, 2, and 3 show very similar spectra, except for small shifts of the frequencies reflecting small differences in the well thicknesses of these samples. The spectra of samples 1 and 2 shown in Figs. 3 and 4 differ somewhat, since they are measured with different dye-laser energies.

Figure 5 shows Raman spectra measured with different laser wavelengths of sample 5 which has GaAs wells of $N=10\pm1$ monolayer thickness. The indicated error (±1) represents the present day state of the art of sample growth. Spectrum (a) is for a laser energy of 1.933 eV and shows very narrow and strong Raman signals corre-

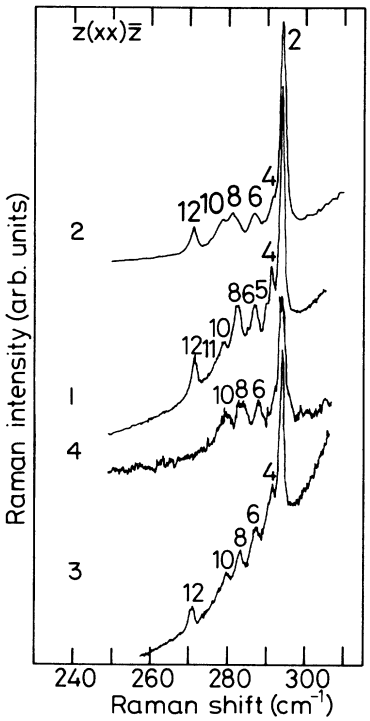

FIG. 4. Raman spectra of the confined LO_{GaAs} phonons in GaAs/AlAs quantum-well samples 1, 2, 3, and 4. Sample 4 is grown deliberately without growth interruption at the top interface—showing the influence of interface roughness on the Raman spectra of the confined LO phonons.

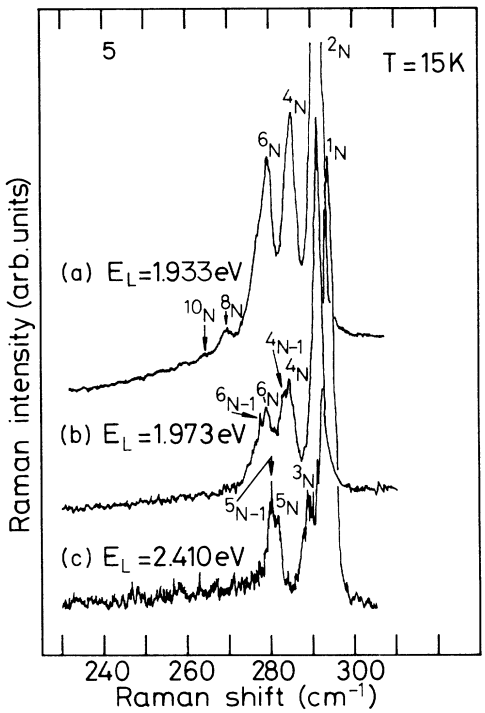

FIG. 5. Raman spectra of a $GaAs_N/AlAs_N$ quantum well (sample 5) with $N=10\pm1$ monolayers. (a) Raman spectrum measured with laser energy $E_L=1.933$ eV. (b) Raman spectrum measured with laser energy $E_L=1.973$ eV. At this slightly higher energy resonance is closer to excitons confined in sections with narrower thickness. Therefore Raman signals from phonons confined in sections with $N-1$ monolayers can also be seen. (c) Raman spectrum measured with 5145-Å Argon laser line. This spectrum shows the scattering due to deformation-potential scattering and therefore predominantly the confined modes of odd order. Spectra (a) and (b) are taken in $z(xx)\bar{z}$ polarization configuration, while spectrum (c) is taken in $z(xy)\bar{z}$ configuration.

sponding to the LO modes for $n=2$, 4, 6, and 8. In addition there is a weaker signal which we assign to the $n=10$ mode. Spectrum (b) is measured under the same conditions except that the dye-laser energy is 1.973 eV, i.e., 40 meV higher than the laser energy for spectrum (a). The higher dye-laser energy for spectrum (b) will bring the resonance closer to an excitonic energy corresponding to a layer thickness decreased by one monolayer and hence we see additional Raman peaks on the shoulder of the peaks occurring in spectrum (a). Thus the additional peaks in spectrum (b) correspond to the LO phonons confined in the regions with $N-1=9$ (± 1) monolayer thickness. This situation is very similar to the case of luminescence, where also luminescence peaks corresponding to regions with thicknesses differing by exactly one monolayer are found (see Fig. 1 and also Refs. 25 and 26). In Fig. 5(c) we show a Raman spectrum in the LO region measured on the same sample but with the 5145-Å (=2.41 eV) Argon laser line. In this case coupling is by deformation-potential coupling to the modes $n=1$, 3, and 5 as explained by Sood *et al.*[8] We observe confined phonon modes from regions with a thickness of $N=10\pm 1$ and $N-1=9\pm 1$ monolayers. By observing the Raman peaks corresponding to thicknesses differing just by one monolayer a very accurate assignment of the Raman energies to specific layer thicknesses can in principle be achieved.

V. LO PHONON DISPERSION

Using the assignment of the observed Raman peaks from the confined LO phonon modes as discussed in the previous section, we compare the confined phonon energies with the bulk dispersion. The comparison of the dispersion of the confined superlattice LO-phonon modes with the dispersion of the bulk GaAs phonons has recently given rise to considerable controversy. Sood *et al.*[8] found that the confined phonon energies for higher orders of confinement deviated considerably to the high-energy side of the bulk LO phonon dispersion. Jusserand *et al.*[16] pointed out that the width of the phonon well is one monolayer wider than the stoichometric width. This argument leads to a correction which is small for wide quantum wells, but becomes very important for thin wells, such as those of Sood *et al.*[8] This correction decreases the above-mentioned discrepancy, but does not remove it. Molinari *et al.*[37] and Strauch and Dorner[38] calculated the dispersion of the confined phonon modes for specific short-period GaAs/AlAs superlattices and found that it is expected to lie very close to the bulk phonon dispersion. Subsequently the bulk phonon dispersion was remeasured with high precision recently at low temperature ($T=10$ K).[15,38] This new measurement agrees largely with older neutron data,[39] which were previously used. The discrepancy remained. We will show below that we believe that this discrepancy is due to thickness fluctuations and interface roughness. It should be kept in mind that in comparing Raman and neutron data, Sood *et al.*[8] shifted the neutron data by a constant amount to achieve agreement at $k=0$.

The dispersion of confined phonons in GaAs/AlAs superlattices for $n=4$, 6, and 8 monolayer thickness has recently been measured at room temperature by Wang, Jiang, and Ploog.[18] These room-temperature data show much better agreement between confined superlattice phonon energies and bulk phonon dispersion. It should be noted, however, that these data show an interesting deviation to higher energies for the highest-order confined phonon modes, i.e., for wave vectors $k>(0.80)2\pi/a_0$. We will discuss this feature in detail in the next section. We attribute this deviation to the effect of interface roughness.

In Fig. 6 we plot the energies of the confined phonon modes for our samples against the confinement wave vector following the analysis of Jusserand *et al.*[16] The solid curve shows the recent neutron scattering results of the LO-phonon dispersion in bulk GaAs. The horizontal error bars show the error in determining the confinement wave vector k due to the uncertainty in the well thickness as a consequence of the interface roughness. Also shown in Fig. 6 are the data of Sood *et al.*[8] where the deviation to higher energies is clearly visible. It should be stressed here that to arrive at Fig. 6 we have made no vertical adjustment of the neutron data (which are taken straight from Ref. 15) nor of the Raman data. Figure 6 compares experimental data without adjustment.

Our work therefore shows that at low temperatures the dispersion of the confined quantum-well LO-phonons

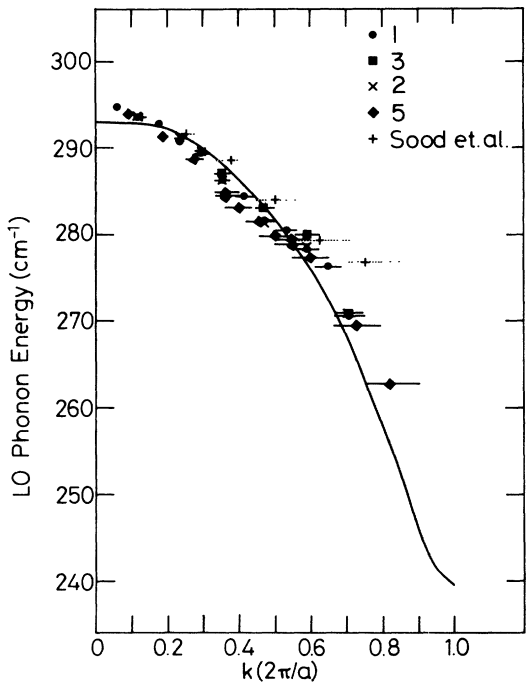

FIG. 6. Energy of the confined LO_{GaAs} phonon modes as a function of confinement wave vector. This dispersion shows close agreement with the phonon dispersion measured recently by neutron scattering for bulk GaAs (solid curve) (Refs. 15 and 17). [The recent neutron measurement agrees closely with older neutron data (Ref. 39)]. Data from Sood *et al.* (Refs. 8, 16, and 17) are also included in this figure. Neutron data (solid curve) are at $T=10$ K, Raman data are at $T=15\pm 2$ K.

agrees with the bulk LO-phonon dispersion within the limits imposed by today's sample growth. Thus we confirm for low temperatures the room-temperature results of Ref. 18.

VI. INFLUENCE OF INTERFACE ROUGHNESS ON CONFINED LO PHONONS

Understanding the influence of interface roughness on the properties of confined phonons is important for two reasons. Firstly it will allow one to obtain information on interface roughness from phonon Raman measurements. Secondly, interface roughness gives rise to errors in comparing the dispersion of confined phonons in quantum wells with the bulk-phonon dispersion. In Refs. 19, 20, and 21 the effect of interface broadening due to thermal interdiffusion[19,20] and the absence of growth interruption[21] has been studied. Jusserand *et al.*[19] show that a diffuse interface leads to a parabolic distortion of the well confining the phonons, resulting in a linear dispersion of the confined phonon modes. Clearly, this treatment is more suitable for conditions where the coherence length of the interface roughness is smaller than the characteristic coherence length of the phonons. Thermal interdiffusion or absence of growth interruption is believed to lead to such short-range interface roughness. Little information is presently available on the coherence length of phonons in quantum wells. In Fig. 5 we have shown phonon modes attributed to sections of the quantum wells with well thicknesses differing by one monolayer. This measurement may indicate that phonons have a similar localization length as excitons. The difficulty in the assignment is that coupling of Raman light to the phonons also plays a role and that we have studied a multiple-quantum-well sample structure, so that signals from different layers may contribute.

We propose an analysis below, which investigates the influence of long-range interface roughness on phonon modes, where the coherence length of smooth interface areas is several thousands of Å or more, as achieved in today's high-quality MBE or MEE samples. When confined phonon energies are plotted against the confinement wave vector, such as in Fig. 6, two effects determine the errors due to roughness and interface thickness uncertainties.

(i) As the confinement wave vector $k_N(n)$ and the order n of the confined phonons increase, the value of $k_N(n)$ becomes increasingly more sensitive to the well thickness Na, where N is the number of monolayers in the phonon well and a is the thickness of one monolayer ($a=2.83$ Å in GaAs).

(ii) The value of the derivative of the LO-phonon dispersion increases strongly as the order n and $k_N(n)$ increase towards the Brillouin-zone boundary.

Consider a phonon mode of order n in a quantum well with a thickness of N monolayers. The confinement wave vector for this mode is[16]

$$k_N(n)=\frac{n\pi}{(N+1)a}, \quad \text{where } 1\le n\le N \tag{1}$$

and where a is the monolayer thickness ($a=2.83$ Å for GaAs). The change in the confinement wave vector $k_N(n)$ for a confined phonon, when the well thickness is changed by one monolayer, is

$$\frac{\Delta k_N(n)}{\Delta N}=-n\frac{\pi}{(N+1)^2a} . \tag{2}$$

The change in $k_N(n)$ due to change of the thickness of the well by one monolayer therefore increases linearly with the order of the confined phonon modes; i.e., the error is small for the $n=1$ mode and very large (approaching the separation of modes of different orders) for high-order n close to N [i.e., for $k_N(n)$ near the Brillouin-zone boundary of the bulk crystal].

Figure 7(a) shows the dependence of $\Delta k_N(n)/\Delta N$ as a function of wave vector. The upper (positive) half shows the decrease in wave vector for an increase of well thickness ($\Delta N=+1$):

$$\Delta k_N(n)/\Delta N=k_{N+1}(n)-k_N(n) . \tag{3}$$

The lower half (negative values) shows the increase in wave vector for a decrease of well thickness by one monolayer ($\Delta N=-1$). In addition to this effect, the slope of the LO-phonon dispersion in GaAs increases as k varies from $k=0$ towards the Brillouin-zone boundary. Therefore the change ΔE of the expected energy of a particular confined phonon mode of order n as a result of a change ΔN in layer thickness Na increases strongly with order n. Figure 7(b) shows this change in energy of the confined phonons of a given order n due to change in well thickness: the upper half (positive values) shows the increase in the energy ΔE of a confined phonon mode when the well thickness is increased by one monolayer ($\Delta N=+1$) against the original value of the wave vector of this confined phonon. The lower half (negative values) shows the equivalent decrease in confined phonon energy when the well thickness is decreased by one monolayer ($\Delta N=-1$). Figure 7(b) shows that the increase of $\Delta k/\Delta N$ and the increase of the slope of the phonon dispersion with increasing wave vector and increasing order of the confined phonons amplify each other. For higher k and n the energy of a confined phonon of a particular order becomes strongly dependent on variations in well thickness. Figure 7(b) also show that this dependence increases with decreasing well width, as expected, since the fractional change in well thickness corresponding to one-monolayer increases, the fewer monolayers there are in total.

Therefore, when determining the phonon dispersion from confined phonon modes much stronger errors are expected for higher-order confined phonon modes with confinement wave vectors closer to the zone boundary. This uncertainty becomes larger the thinner the quantum wells are. To determine the phonon dispersion from Raman measurements in quantum wells, therefore the low-index confined phonons in thicker wells are best. We believe that our present combination of thicknesses are therefore a good choice. Figure 7(b) clearly demonstrates this dependence of error on thickness N and mode order n. Thus we believe that the errors of the present experimental phonon dispersion are smaller than in measure-

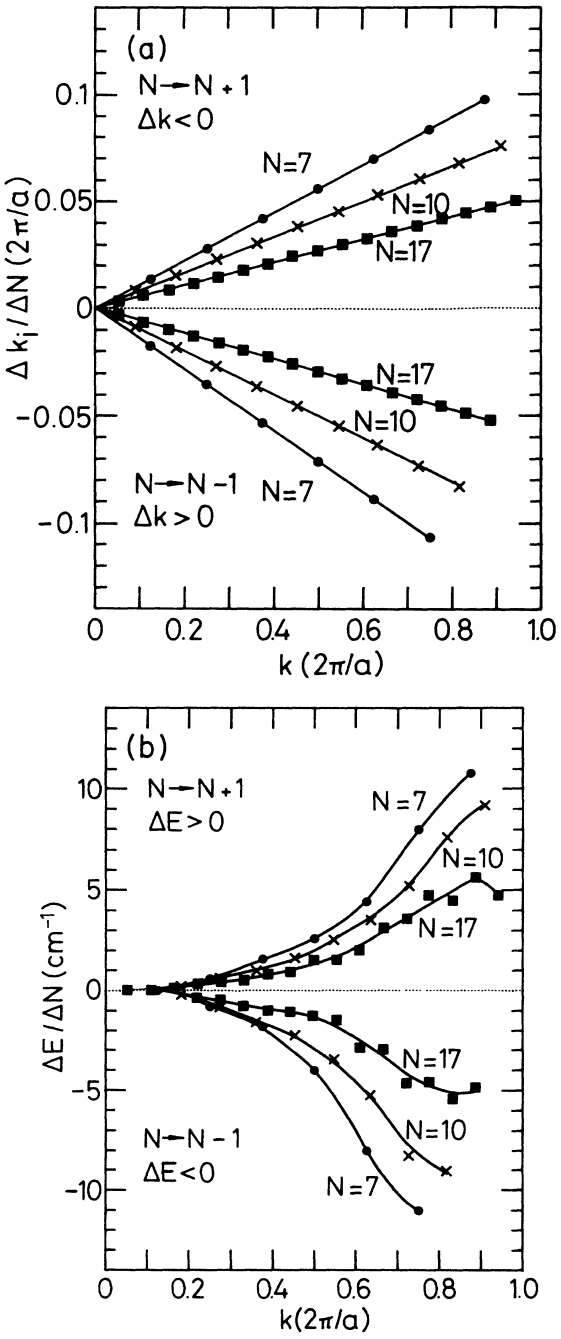

FIG. 7. (a) This figure shows the dependence of the confinement wave vector of phonons on a change in thickness of the quantum well by one monolayer. The upper half (positive $\Delta k/\Delta N$) shows the decrease of k_n upon increase of the well thickness by one monolayer ($\Delta N=+1$). The lower half (negative $\Delta k/\Delta N$) shows the increase of k_n upon decrease of the well thickness by one monolayer ($\Delta N=-1$). This figure demonstrates that roughness with "long" correlation length (see text) has stronger influence on higher-order confined modes than on modes with k close to zero. (b) Change ΔE in energy of the confined LO-phonon mode upon change of well thickness by one monolayer. The upper half (positive $\Delta E/\Delta N$) shows the increase of energy of a particular phonon mode n upon increase of well thickness by one monolayer ($\Delta N=+1$). The lower half (negative $\Delta E/\Delta N$) shows the decrease of well thickness by one monolayer ($\Delta N=-1$).

ments using thinner wells.

Previous determinations[8,17,18] of phonon dispersion from Raman measurements, show deviations from the bulk phonon dispersion for high orders of the confined phonon modes [for $k>(0.7)2\pi/a_0$ in Refs. 16 and 17, and $k>(0.8)2\pi/a_0$ in Ref. 18]. The data of Sood *et al.*[17] are included in Fig. 6, where we have added error bars (dotted horizontal bars) assuming thickness fluctuations and uncertainties of plus or minus one monolayer. Clearly, thickness fluctuations or errors of the order of one monolayer can explain the discrepancies. It should be noted that the samples of Ref. 8 and Ref. 17 were grown without growth interruption. Figure 7(b) allows one to estimate the amplitude of the interface uncertainties to be around plus or minus one monolayer.

Sample 4 is grown without growth interruption at the top interface. We do not find Raman scattering by the confined phonon mode $n=12$ or any higher-order mode as apparent from the spectra shown in Fig. 4. In the other samples 1, 2, and 3 the absence of a Raman signal for phonon modes of order greater than 12 may be attributed to disorder as well. It is striking that for the samples 1, 2, and 3 the modes $n=4$ to 12 have very similar Raman intensity, while all higher modes are too weak to be observed, i.e., their scattering cross section is at least a factor of 5 lower. This fact is surprising at first and it is unlikely to be caused by the different Raman scattering efficiencies of modes 1–12 as opposed to modes 13–17 alone. We believe it is more plausible that the phonon modes change character as the energy shift due to interface fluctuations increases as the mode index increases [see Fig. 7(b)]. Thus for a well with 17 monolayers the energy change due to a thickness change of $\Delta N=1$ exceeds 3 meV (the phonon line width) for $n>12$ [see fig. 7(b)]. It also exceeds the band widths of the dispersion of the confined LO phonons parallel to the wells, which is around 2 meV.[14,15] The $\Delta E/\Delta N$ value for sample 5 ($N=10\pm1$ monolayers) is also less than about 3 meV when n is less than 6. This explains consistently the absence (or suppression) of Raman peaks for n greater than 6 in Fig. 5 as a consequence of roughness. Thus we expect there is a distinct possibility of localization of the phonons parallel to the wells due to interface disorder, similar to Anderson localization of electrons. Indeed, we do not observe phonon modes above $n=12$.

VII. CONCLUSIONS

We have studied Raman scattering in double resonance by confined LO-phonon modes in a series of GaAs/AlAs quantum wells which were grown by refined MBE with growth interruption at the interfaces and other samples grown by migration enhanced epitaxy (MEE). Thus we have studied wells with very smooth interfaces, as demonstrated by the luminescence spectra. We have observed the confined LO-phonon modes in these GaAs wells up to the order $n=12$. The polarization dependences are those expected for double resonance. We plot the energies of the confined LO_{GaAs} phonon modes as a function of confinement wave vector. We find good agreement of this dependence with recent neutron

scattering measurements of the bulk LO-phonon dispersion in GaAs. We do not find the discrepancy previously reported in Refs. 8, 16, 17 between the dispersion of confined phonons and the bulk phonon dispersion. We examine in detail the errors arising from long-range interface roughness and well thickness uncertainties on the determination of the phonon dispersion. We argue that the previously found discrepancies at high order of confined phonons are due to interface roughness and associated uncertainty in the well thickness. We show that roughness, fluctuations and uncertainties in the thickness have a much stronger effect on higher order confined phonons. The energy of confined phonons of order n depends much more strongly on a thickness change by one monolayer, the larger n and the smaller the well thickness Na is (a is the thickness of one monolayer; $a=2.83$ Å in GaAs).

Thus for determination of the phonon dispersion, Raman measurements of low-order phonons in quantum wells of intermediate thickness are optimal. Thus our samples represent a good choice for determination of the phonon dispersion. On the other hand, to characterize the roughness of interfaces it is necessary to use the high-order confined phonons, since the low-order phonons are fairly insensitive to thickness fluctuations. The intuitive reason is that low-order phonons have a small vibrational amplitude near the interface, and are therefore not expected to be strongly dependent on the properties of the interface. In high-quality wells with a thickness of 17 monolayers we observe phonons up to $n=12$. In a quantum well grown without growth interruption at the top interface on the other hand, we only observe modes up to $n=10$ in Raman scattering. By consulting Fig. 7(b) we attribute this absence of higher modes to interface roughness, since it is unlikely that the dependence of the Raman cross section on the mode order alone should lead to such an abrupt drop in cross section between phonon modes for $n \leq 10$ and $n \geq 12$.

ACKNOWLEDGMENTS

One of the authors (G.F.) would like to express his deep gratitude to the Institute for Physical and Chemical Research (RIKEN–Wako-shi, Saitama), and to the Institute of Industrial Science of the University of Tokyo and their employees for the support of this work, for many helpful discussions, and for the kind hospitality. G. F. greatfully acknowledges helpful discussions and support of this work by Y. Aoyagi. We would like to thank Kazuhiko Hirakawa, Toshio Matsusue, and Hisao Yoshimura for many discussions and much help in performing this work. The work is partly supported by the Frontier Material Project of RIKEN and by a Grant-in-Aid from the Ministry of Education, Science and Culture, Japan. We express our gratitude to B. Jusserand and M.-H. Meynadier for sending us manuscripts prior to publication. Helpful discussions with U. Ekenberg and B. Jusserand are gratefully acknowledged.

*Permanent address: Cavendish Laboratory, University of Cambridge, Madingley Road, Cambridge CB3 0HE, England.

[1]M. V. Klein, IEEE J. Quantum Electron **QE-22**, 1760 (1986).

[2]J. M. Worlock, in *Proceedings of the Second International Conference on Phonon Physics,* edited by J. Kollár, N. Kroó, N. Menyhárd, and T. Siklós (World Scientific, Singapore, 1985), p. 506.

[3]M. Cardona, in *Lectures on Surface Science,* Proceedings of the Fourth Latin-American Symposium, edited by G. R. Castro and M. Cardona (Springer-Verlag, Berlin, 1987), p. 2.

[4]B. Jusserand and M. Cardona (unpublished).

[5]C. Colvard, K. Merlin, M. V. Klein, and A. C. Gossard, Phys. Rev. Lett. **45**, 298 (1980).

[6]C. Colvard, T. A. Grant, M. V. Klein, R. Merlin, R. Fisher, H. Morkoç, and A. C. Gossard, Phys. Rev. B **31**, 2080 (1985).

[7]B. Jusserand, D. Paquet, and A. Regreny, Phys. Rev. B **30**, 6245 (1984).

[8]A. K. Sood, J. Menéndez, M. Cardona, and K. Ploog, Phys. Rev. Lett. **54**, 2111 (1985).

[9]A. K. Sood, J. Menéndez, M. Cardona, and K. Ploog, Phys. Rev. Lett. **54**, 2115 (1985).

[10]A. Fasolino, E. Molinari, and J. C. Maan, Phys. Rev. B **33**, 8889 (1986).

[11]E. Molinari, A. Fasolino, and K. Kunc, Phys. Rev. Lett. **56**, 1751 (1986).

[12]B. Jusserand and D. Paquet, in *Semiconductor Superlattices and Heterojunctions,* edited by N. Boccara (Springer-Verlag, Berlin, 1986), p. 108.

[13]B. Zhu and K. A. Chao, Phys. Rev. B **36**, 4906 (1987).

[14]Shang-Fen Ren, Hanyou Chu, and Yia-Chung Chang, Phys. Rev. Lett. **59**, 1841 (1987).

[15]E. Richter and D. Strauch, Solid State Commun. **64**, 867 (1987).

[16]B. Jusserand and D. Paquet, Phys. Rev. Lett. **56**, 1752 (1986).

[17]A. K. Sood, J. Menéndez, M. Cardona, and K. Ploog, Phys Rev. Lett. **56**, 1753 (1986).

[18]Z. P. Wang, D. S. Jiang, and K. Ploog, Solid State Commun. **65**, 661 (1988).

[19]B. Jusserand, F. Alexandre, D. Paquet, and G. Le Roux, Appl. Phys. Lett. **47**, 301 (1985).

[20]D. Levi, Shu-Lin Zhang, M. V. Klein, J. Klem, and H. Morkoç, Phys. Rev. B **36**, 8032 (1987).

[21]G. W. Wicks, J. T. Bradshaw, and D. C. Radulescu, Appl. Phys. Lett. **52**, 570 (1988).

[22]H. Sakaki, M. Tanaka, and J. Yoshino, Jpn. J. Appl. Phys. **24**, L417 (1985).

[23]Y. Horikoshi, M. Kawashima, and H. Yamaguchi, Jpn. J. Appl. Phys. **25**, L868 (1986).

[24]Y. Horikoshi, M. Kawashima, and H. Yamaguchi, Jpn. J. Appl. Phys. **27**, 169 (1988).

[25]M. Tanaka, H. Sakaki, and J. Yoshino, Jpn. J. Appl. Phys. **25**, L155 (1986).

[26]M. Tanaka, H. Sakaki, J. Yoshino, and T. Furuta, Surf. Sci. **174**, 65 (1986).

[27]A. Ishibashi, Y. Mori, M. Itabashi, and N. Watanabe, J. Appl. Phys. **58**, 2691 (1985).

[28]E. Finkman, M. D. Sturge, M.-H Meynadier, R. E. Nahory, M. C. Tamargo, D. M. Hwang, and C. C. Chang, J. Lumin. (to be published).
[29]K. J. Moore, P. Dawson, and C. T. Foxon, J. Phys. (Paris) Colloq. **48**, C5-525 (1987).
[30]G. Danan, B. Etienne, F. Mollot, R. Planel, A. M. Jean-Louis, F. Alexandre, B. Jusserand, G. Le Roux, J. Y. Marzin, H. Savary, and B. Sermage, Phys. Rev. B **35**, 6207 (1987).
[31]J. L. de Miguel, K. Fujiwara, L. Tapfer, and K. Ploog, Appl. Phys. Lett. **47**, 836 (1985).
[32]J. N. Schulman and T. C. McGill, Phys. Rev. B **19**, 6341 (1979).
[33]G. Bastard, Phys. Rev. B **24**, 5693 (1981).
[34]R. C. Miller, D. A. Kleinman, and A. C. Gossard, Solid State Commun. **60**, 213 (1986).
[35]R. C. Miller, D. A. Kleinman, and A. C. Gossard, Phys. Rev. B **34**, 7444 (1986).
[36]D. A. Kleinman, R. C. Miller, and A. C. Gossard, Phys. Rev. B **35**, 664 (1987).
[37]E. Molinari, A. Fasolino, and K. Kunc, in *Proceedings of the 18th International Conference on the Physics of Semiconductors,* edited by O. Engström (World Scientific, Singapore, 1987), p. 663.
[38]D. Strauch and B. Dorner (unpublished).
[39]J. L. T. Waugh and G. Dolling, Phys. Rev. **132**, 2410 (1963).